JOC Article

A New Solvent-Dependent Mechanism for a Triazolinedione Ene Reaction

Orlando Acevedo* and Michael E. Squillacote*

Department of Chemistry and Biochemistry, Auburn University, Auburn, Alabama 36849

orlando.acevedo@auburn.edu; squilme@auburn.edu

Received October 11, 2007

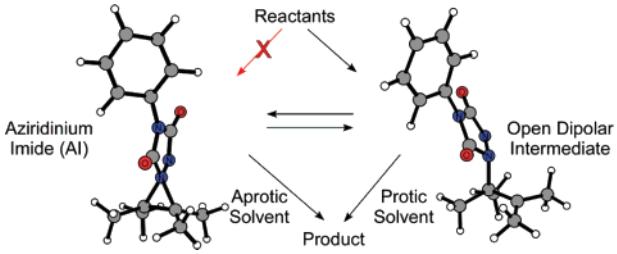

The ene reaction between 4-phenyl-1,2,4-triazoline-3,5-dione (PTAD) and tetramethylethylene has been investigated using QM/MM calculations in water, methanol, DMSO, and acetonitrile. The effects of solvation on the mechanism and rates of reaction are elucidated using two-dimensional potentials of mean force (PMF) simulations utilizing free-energy perturbation theory and Monte Carlo statistical mechanics. A new mechanism is proposed where direct formation of an open dipolar intermediate following the addition of PTAD to the alkene is rate-limiting and the pathway toward ene product is significantly dependent on the reaction medium. In protic solvents, the open dipolar intermediate may proceed directly to the ene product or reversibly form an aziridinium imide (AI) intermediate that does not participate in the reaction. However, in aprotic solvents the open intermediate is short-lived ($<10^{-11}$ s) and the ene product forms via the AI intermediate. The calculated free energies of activation are in close agreement with those derived from experiment, e.g., $\Delta G^{\ddagger}$ of 14.9 kcal/mol compared to 15.0 kcal/mol in acetonitrile. Density functional theory calculations at the (U)B3LYP/6-311++G(2d,p) level using the CPCM continuum solvent model were also carried out and confirmed a zwitterionic, and not diradical, open intermediate present in the reaction. Only the QM/MM methodology was able to accurately reproduce the experimental rates and differentiate between the protic and aprotic solvents. Solute−solvent interaction energies, radial distribution functions, and charges are analyzed and show that the major factor dictating the changes in reaction path is hydrogen bond stabilization of the charge separations spanning 2 to 4 atoms in the intermediates and transition states.

Introduction

The ene reaction involving the highly reactive electrophile triazolinedione has drawn considerable attention for its synthetic utility[1] and controversial mechanism—the subject of numerous experimental[2−11] and theoretical studies.[12,13] Initially believed to proceed via a concerted pericyclic mechanism,[14] the addition of an electrophilic double bond to an alkene with a concomitant allylic hydrogen transfer, kinetic isotope effects,[2,7,8] and solvent trapping experiments[5,8] have established that the reaction follows a stepwise route. However, several issues concerning the

(1) (a) Baran, P. S.; Guerrero, C. A.; Corey, E. J. *J. Am. Chem. Soc.* **2003**, *125*, 5628−5629. (b) Baran, P. S.; Guerrero, C. A.; Corey, E. J. *Org. Lett.* **2003**, *5*, 1999−2001. (c) Adam, W.; Degen, H.-G.; Krebs, O.; Saha-Möller, C. R. *J. Am. Chem. Soc.* **2002**, *124*, 12938−12939. (d) Gau, A.-H.; Lin, G.-L.; Uang, B.-J.; Liao, F.-L.; Wang, S.-L. *J. Org. Chem.* **1999**, *64*, 2194−2201.

(2) Seymour, C. A.; Greene, F. D. *J. Am. Chem. Soc.* **1980**, *102*, 6384−6385.

(3) (a) Hall, J. H.; Jones, M. L. *J. Org. Chem.* **1983**, *48*, 822−826. (b) Elemes, Y.; Orfanopoulos, M. *Tetrahedron Lett.* **1991**, *32*, 2667−2670. (c) Adam, W.; Bottke, N.; Krebs, O.; Lykakis, I.; Orfanopoulos, M.; Stratakis, M. *J. Am. Chem. Soc.* **2002**, *124*, 14403−14409. (d) Kim, D. K.; O'Shea, K. E. *J. Am. Chem. Soc.* **2004**, *126*, 700−701. (e) Syrgiannis, Z.; Elemes, Y. *Tetrahedon Lett.* **2006**, *47*, 2961−2964. (f) Syrgiannis, Z.; Elemes, Y. *Tetrahedon Lett.* **2006**, *47*, 6831−6834.

(4) Cheng, C.-C.; Seymour, C. A.; Petti, M. A.; Greene, F. D.; Blount, J. F. *J. Org. Chem.* **1984**, *49*, 2910−2916.

(5) Smonou, I.; Orfanopoulos, M.; Foote, C. S. *Tetrahedon Lett.* **1988**, *29*, 2769−2772.

10.1021/jo7022153 CCC: $40.75
Published on Web 12/28/2007

SCHEME 1. Possible Ene Reaction Pathways for 4-Phenyl-1,2,4-triazoline-3,5-dione (PTAD) and Tetramethylethylene

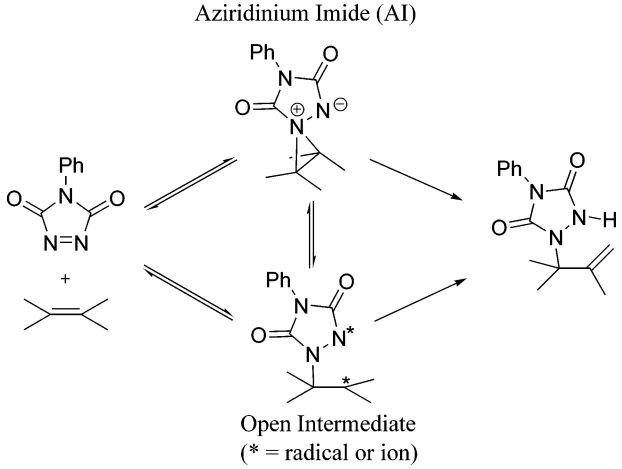

mechanistic pathway remain unresolved, e.g., the stabilities and roles played by two intermediates: an aziridinium imide (AI) and either an open biradical or dipolar (zwitterion) intermediate (Scheme 1).

Traditionally, triazolinedione−alkene reactions have been accepted to proceed via the rate-limiting formation of an AI intermediate that leads directly to products;[2,7,8,12] spectroscopic observations of the AI lent support for the mechanism.[6,9,15] However, a combined experimental and computational study by Singleton and Hang called the established mechanism into question by suggesting a rapid equilibrium between the AI and open biradical intermediates where only the biradical proceeded to form the ene product.[13] Subsequent investigations have both challenged the controversial biradical mechanism on the basis of stereoisotopic and product studies[10] and lent it support through the characterization of photochemically generated AI intermediates.[16] A recent study by Roubelakis et al. has further contributed to the complexity of the triazolinedione−alkene mechanism by proposing a solvent dependency; in the aprotic solvents ($CDCl_3$, CH_2Cl_2, acetone, acetonitrile, and DMSO) the ene adducts are reported to form via an AI pathway, whereas in protic solvents (methanol and ethanol) an open dipolar, not biradical, intermediate route prevailed.[11]

To explore the effect of solvent on the ene mechanism and intermediate stabilities, the reaction between 4-phenyl-1,2,4-triazoline-3,5-dione (PTAD) and tetramethylethylene has been investigated using mixed quantum and molecular mechanics (QM/MM) simulations. This specific reaction was chosen in light of the extensive experimental data available and for the olefin's sensitivity toward solvent polarities.[4,14] Reactants, intermediates, transition structures, and products have been located in four different solvents: water, methanol, DMSO, and acetonitrile. Activation barriers were computed with complete sampling of the geometry of the reacting systems and explicit representation of the solvent molecules. Changes in solvation along reaction paths are fully characterized. Comparisons are made to results from density functional theory (DFT) calculations with the CPCM implicit solvation model.

The results presented provide new insights as to the solvent effects on the reaction pathways and help to weave a resolution to unexplained/contradictory observations. The initial addition of PTAD to the alkene is computed to be the rate-determining step and to proceed solely to the open intermediate in all solvents. A rapid equilibrium between the AI and open intermediates is predicted to occur more readily in the protic solvents compared to the aprotic ones, and the AI intermediate was computed to be significantly more stable than the open intermediate in both types of solvent. The simulations find the pathway to the final ene product is dictated by the choice of solvent—the hydrogen abstraction occurs via the AI intermediate in aprotic solvents, but an open intermediate is responsible for this final step in protic solvents. Large charge separations calculated for the open intermediate indicate a dipolar, and not a biradical, structure. These results provide additional insight to the reaction mechanism and have broad implications toward the mechanisms of related ene reactions, including the singlet oxygen ($^1O_2$)[8,17] and nitrosoarene (ArNO)[18] systems.

Computational Methods

QM/MM calculations,[19] as implemented in BOSS 4.6,[20] were carried out with the reacting system treated using the PDDG/PM3 semiempirical molecular orbital method.[21] PDDG/PM3 has been extensively tested for gas-phase structures and energetics,[22] and has given excellent results in solution-phase QM/MM studies for a wide variety of organic and enzymatic reactions.[23−27] The solvent

(6) Squillacote, M.; Mooney, M.; De Felippis, J. *J. Am. Chem. Soc.* **1990**, *112*, 5364−5365.
(7) Orfanopoulos, M.; Smonou, I.; Foote, C. S. *J. Am. Chem. Soc.* **1990**, *112*, 3607−3614.
(8) Smonou, I.; Khan, S.; Foote, C. S.; Elemes, Y.; Mavridis, I. M.; Pantidou, A.; Orfanopoulos, M. *J. Am. Chem. Soc.* **1995**, *117*, 7081−7087.
(9) Poon, T. H. W.; Park, S. H.; Elemes, Y.; Foote, C. S. *J. Am. Chem. Soc.* **1995**, *117*, 10468−10473.
(10) (a) Vassilikogiannakis, G.; Elemes, Y.; Orfanopoulos, M. *J. Am. Chem. Soc.* **2000**, *112*, 9540−9541. (b) Vassilikogiannakis, G.; Stratakis, M.; Orfanopoulos, M. *Org. Lett.* **2000**, *2*, 2245−2248. (c) Stratakis, M.; Hatzimarinaki, M.; Froudakis, G. E.; Orfanopoulos, M. *J. Org. Chem.* **2001**, *66*, 3682−3687.
(11) Roubelakis, M. M.; Vougioukalakis, G. C.; Angelis, Y. S.; Orfanopoulos, M. *Org. Lett.* **2006**, *8*, 39−42.
(12) Chen, J. S.; Houk, K. N.; Foote, C. S. *J. Am. Chem. Soc.* **1997**, *119*, 9852−9855.
(13) Singleton, D. A.; Hang, C. *J. Am. Chem. Soc.* **1999**, *121*, 11885−11893.
(14) Ohashi, S.; Butler, G. B. *J. Org. Chem.* **1980**, *45*, 3472−3476.
(15) Nelsen, S. F.; Kapp, D. L. *J. Am. Chem. Soc.* **1985**, *107*, 5548−5549.
(16) Squillacote, M.; Garner, C.; Oliver, L.; Mooney, M.; Lai, Y.-L. *Org. Lett.* **2007**, *9*, 5405−5408.
(17) Singleton, D. A.; Hang, C.; Szymanski, M. J.; Meyer, M. P.; Leach, A. G.; Kuwata, K. T.; Chen, J. S.; Greer, A.; Foote, C. S.; Houk, K. N. *J. Am. Chem. Soc.* **2003**, *125*, 1319−1328.
(18) (a) Seymour, C. A.; Greene, F. D. *J. Org. Chem.* **1982**, *47*, 5226−5227. (b) Adam, W.; Krebs, O.; Orfanopoulos, M.; Stratakis, M.; Vougioukalakis, G. C. *J. Org. Chem.* **2003**, *68*, 2420−2425. (c) Leach, A. G.; Houk, K. N. *Org. Biomol. Chem.* **2003**, *1*, 1389−1403. (d) Adam, W.; Krebs, O. *Chem. Rev.* **2003**, *103*, 4131−4146.
(19) (a) Aqvist, J.; Warshel, A. *Chem. Rev.* **1993**, *93*, 2523−2544. (b) Gao, J. *Acc. Chem. Res.* **1996**, *29*, 298−305. (c) Kaminski, G. A.; Jorgensen, W. L. *J. Phys. Chem. B* **1998**, *102*, 1787−1796.
(20) Jorgensen, W. L.; Tirado-Rives, J. *J. Comput. Chem.* **2005**, *26*, 1689−1700.
(21) (a) Repasky, M. P.; Chandrasekhar, J.; Jorgensen, W. L. *J. Comput. Chem.* **2002**, *23*, 1601−1622. (b) Tubert-Brohman, I.; Guimarães, C. R. W.; Repasky, M. P.; Jorgensen, W. L. *J. Comput. Chem.* **2003**, *25*, 138−150. (c) Tubert-Brohman, I.; Guimarães, C. R. W.; Jorgensen, W. L. *J. Chem. Theory Comput.* **2005**, *1*, 817−823.
(22) Sattelmeyer, K. W.; Tirado-Rives, J.; Jorgensen, W. L. *J. Phys. Chem. A* **2006**, *110*, 13551−13559.
(23) Acevedo, O.; Jorgensen, W. L. *Org. Lett.* **2004**, *6*, 2881−2884.
(24) (a) Acevedo, O.; Jorgensen, W. L. *J. Am. Chem. Soc.* **2005**, *127*, 8829−8834. (b) Acevedo, O.; Jorgensen, W. L. *J. Org. Chem.* **2006**, *71*, 4896−4902. (c) Tubert-Brohman, I.; Acevedo, O.; Jorgensen, W. L. *J. Am. Chem. Soc.* **2006**, *128*, 16904−16913.

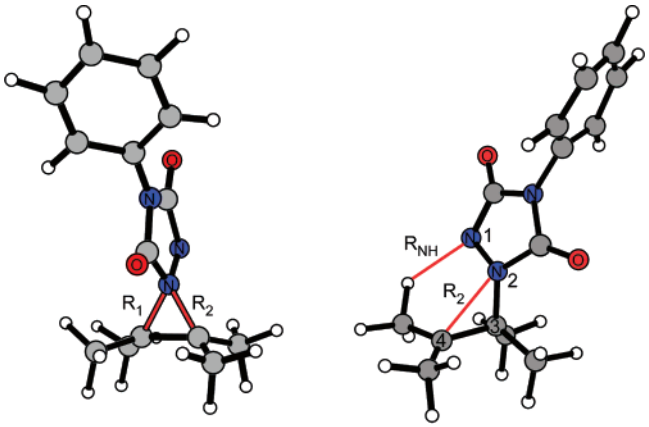

FIGURE 1. Reaction coordinates, R_1 and R_2 (free-energy map 1) and R_{NH} and R_2 (free-energy map 2), for the ene reaction between 4-phenyl-1,2,4-triazoline-3,5-dione (PTAD) and tetramethylethylene. Illustrated structures are the aziridinium imide (AI) intermediate ($R_1 = R_2 = \sim 1.55$ Å) and the transition structure corresponding to the allylic hydrogen abstraction ($TS_{abs.}$) ($R_{NH} = 2.11$ Å, $R_1 = 1.49$ Å, and $R_2 = 2.33$ Å) from aqueous-phase QM/MM simulations using PDDG/PM3.

molecules are represented with the TIP4P water model[28] and the united-atom OPLS force field for the nonaqueous solvents.[29] The systems consisted of the reactants, plus 390 solvent molecules for DMSO and acetonitrile, 595 molecules for methanol, or 730 molecules for water. The systems are periodic and tetragonal with $c/a = 1.5$; a is ca. 25, 29, 31, and 32 Å for water, acetonitrile, DMSO, and methanol. To locate the minima and maxima on the free-energy surfaces, separate 2-dimensional free-energy maps were constructed for each reaction in solution using the lengths of the two forming C−N bonds, R_1 and R_2, as the reaction coordinates for the first free-energy map and R_2 with a hydrogen abstraction coordinate, R_{NH}, for the second map (Figure 1). Free-energy perturbation (FEP) calculations were performed in conjunction with NPT Metropolis Monte Carlo (MC) simulations at 25 °C and 1 atm. The reactant state was defined by $R_1 = R_2 = 5.0$ Å, and the free-energy surfaces were flat in this vicinity.

In the present QM/MM implementation, the solute's intramolecular energy is treated quantum mechanically using PDDG/PM3; computation of the QM energy and atomic charges is performed for each attempted move of the solute, which occurred every 100 configurations. For electrostatic contributions to the solute−solvent energy, CM3 charges[30] were obtained for the solute using PDDG/PM3 calculations with a scaling factor of 1.14. This is augmented with standard Lennard-Jones interactions between solute and solvent atoms using OPLS parameters. This combination is appropriate for a PM3-based method as it minimizes errors in computed free energies of hydration.[31]

Solute−solvent and solvent−solvent intermolecular cutoff distances of 12 Å were employed based on all heavy atoms of the solute, the oxygens of water and methanol, and the central carbon and sulfur atoms of acetonitrile and DMSO. If any distance is within the cutoff, the entire solute−solvent or solvent−solvent interaction was included. Quadratic feathering of the intermolecular interactions within 0.5 Å of the cutoff was applied to soften the discontinuity in energy. Total translations and rotations were sampled in ranges that led to overall acceptance rates of about 40−46% for new configurations. Multiple FEP windows were run simultaneously on a Linux cluster at Auburn University and on computers located at the Alabama Supercomputer Center.

Density functional theory (DFT) calculations at the restricted and unrestricted B3LYP/6-31+G(d)[32] theory level were also used to characterize the transition structures and ground states in vacuum using Gaussian 03.[33] The DFT calculations were used for geometry optimizations and computations of vibrational frequencies, which confirmed all stationary points as either minima or transition structures and provided thermodynamic corrections. The effect of solvent was approximated by subsequent single-point calculations using the conductor-like polarizable continuum model (CPCM)[34] with the UFF cavity model and (U)B3LYP/6-311++G(2d,p) theory level; dielectric constants of 78.39, 32.63, 36.64, and 46.7 were used for water, methanol, acetonitrile, and DMSO.

Results and Discussion

Structures. Recent experimental observations for reactions between cyclopropyl-substituted alkenes with the enophile PTAD provide evidence of mechanistic changes dependent on the choice of solvent;[11] however, previous theoretical work on the ene reaction relied exclusively on gas-phase structures to predict the mechanism.[12,13] In the present study, geometries for the ene reaction in solution were located with the QM/MM/MC calculations by starting from the gas-phase PDDG/PM3 structures and perturbing the two reacting C−N bonds, R_1 and R_2, between PTAD and tetramethylethylene to find the AI and open intermediates and the transition structures associated with the initial addition of PTAD to the alkene, $TS_{add.}$, and the isomerization between the intermediates, $TS_{isomer.}$ (Figure 1). All internal degrees of freedom other than the two reaction coordinates R_1 and R_2 were fully sampled during the simulations. The initial ranges for R_1 and R_2 were 1.45−2.60 Å. Each FEP calculation entailed 5 million (M) configurations of equilibration and 10 M configurations of averaging and was computed using increments of 0.05 Å. The present QM/MM/MC/FEP calculations include extensive sampling of the substrates and hundreds of solvent molecules to obtain configurationally averaged free-energy changes as opposed to energy minimizations, which do not include entropy effects and are sensitive to starting geometries. As an example, the resultant maps for the ene reaction in water and DMSO, which required ca. 500 FEP calculations each, are shown in Figure 2. A second free-energy map (Figure 3), requiring ca. 1000 FEP calculations, used a second set of reaction coordinates, R_2 and R_{NH} (Figure 1) to locate the transition structure corresponding to the allylic proton abstraction, $TS_{abs.}$, the intermediates, and the ene product. The geometries of the AI and open intermediates are identical in both free-energy maps (within the level of uncertainty in the

(25) Acevedo, O.; Jorgensen, W. L. *J. Am. Chem. Soc.* **2006**, *128*, 6141−6146.
(26) Acevedo, O.; Jorgensen, W. L.; Evanseck, J. D. *J. Chem. Theory Comput.* **2007**, *3*, 132−138.
(27) Acevedo, O.; Jorgensen, W. L. *J. Chem. Theory Comput.* **2007**, *3*, 1412−1419.
(28) Jorgensen, W. L.; Chandrasekhar, J.; Madura, J. D.; Impey, W.; Klein, M. L. *J. Chem. Phys.* **1983**, *79*, 926−935.
(29) (a) Jorgensen, W. L. *J. Phys. Chem.* **1986**, *90*, 1276−1284. (b) Jorgensen, W. L.; Briggs, J. M. *Mol. Phys.* **1988**, *63*, 547−558. (c) Jorgensen, W. L.; Briggs, J. M.; Contreras, M. L. *J. Phys. Chem.* **1990**, *94*, 1683−1686. (d) Briggs, J. M.; Matsui, T.; Jorgensen, W. L. *J. Comput. Chem.* **1990**, *11*, 958−971.
(30) Thompson, J. D.; Cramer, C. J.; Truhlar, D. G., *J. Comput. Chem.* **2003**, *24*, 1291−1304.
(31) Udier-Blagovic, M.; De Tirado, P. M.; Pearlman, S. A.; Jorgensen, W. L. *J. Comput. Chem.* **2004**, *25*, 1322−1332.
(32) (a) Becke, A. D. *J. Chem. Phys.* **1993**, *98*, 5648−5652. (b) Lee, C.; Yang, W.; Parr, R. G. *Phys. Rev.* **1988**, *37*, 785−789.
(33) Frisch, M. J.; et al. *Gaussian 03*, Revision D.01; Gaussian, Inc.: Wallingford, CT, 2004.
(34) Cossi, M.; Rega, N.; Scalmani, G.; Barone, V. *J. Comput. Chem.* **2003**, *24*, 669−681.
(35) Orfanopoulos, M.; Foote, C. S.; Smonou, I. *Tetrahedon Lett.* **1987**, *28*, 15−18.

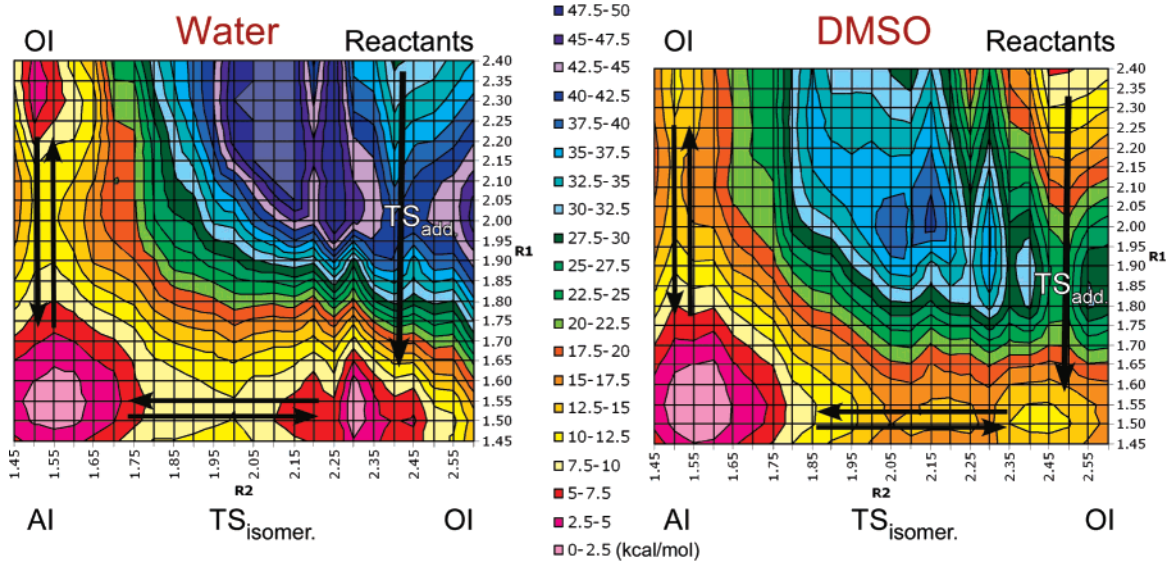

FIGURE 2. Two-dimensional potentials of mean force (free-energy map 1; reaction coordinates R_1 and R_2) for the ene reaction in water and DMSO. AI = aziridinium imide intermediate, OI = open intermediate, $TS_{add.}$ = initial transition state (addition of PTAD), $TS_{isomer.}$ = transition state for isomerization of the intermediates. All distances in angstroms. Maximum free-energy values truncated to 50 kcal/mol for clarity.

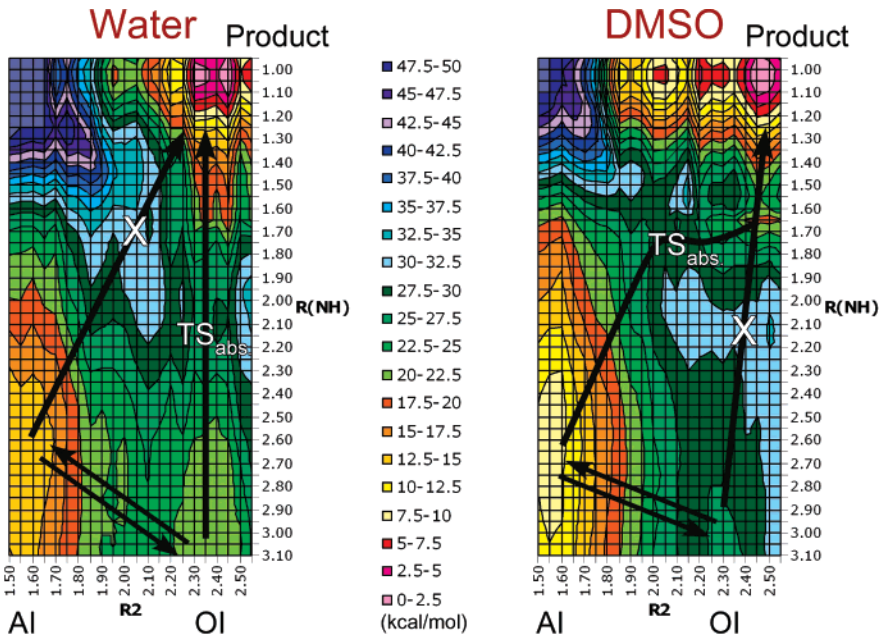

FIGURE 3. Two-dimensional potentials of mean force (free-energy map 2; reaction coordinates R_2 and R_{NH}) for the ene reaction in water and DMSO. $TS_{abs.}$ = transition state for ene product formation (allylic hydrogen abstraction), X = energetically unfavorable reaction path (additional abbreviations and units given in Figure 2).

results, ca. ±0.02 Å after refinement) and are used to link the energy values between the maps. The number of single-point QM calculations used to construct free-energy maps 1 and 2 was ca. 75 and 150 million per solvent, respectively, emphasizing the need for highly efficient QM methods in such studies. Similar maps for methanol and acetonitrile are presented in the Supporting Information (Figures S1 and S2).

To locate the critical points more precisely, the regions surrounding the intermediates and transition states from the initial maps were explored in increments of 0.01 Å. This provided refined results for the reaction geometries in the four solvents, as summarized in Table 1. Optimized transition structures and intermediates for the reaction pathway in aqueous solution are illustrated in Figure 4 and structures in DMSO are given in the Supporting Information (Figure S3). The calculations predict a stepwise mechanism with three transition structures and two intermediates present in the reaction (Figure 5).

The PDDG/PM3 transition structure geometries for the initial addition of PTAD, $TS_{add.}$, show only small changes in reacting bond lengths with values of $R_1 = 1.78-1.84$ Å and $R_2 = 2.45-2.50$ Å in the four solutions and are similar to a previously reported B3LYP/6-31G(d) gas-phase structure, $R_1 = 1.91$ Å and $R_2 = 2.47$ Å, for the reaction between TAD and tetramethylethylene.[13] The QM/MM/MC simulations find the reaction proceeds exclusively to an open intermediate (OI) in all solvents. An intrinsic reaction coordinate (IRC) analysis performed by Singleton and Hang using gas-phase DFT calculations yielded

TABLE 1. Computed Bond Lengths (Å) and Torsion (deg) for the Ene Reaction Structures between PTAD and Tetramethylethylene at 25 °C and 1 atm[a]

	R_1	R_2	R_{NH}	ϕ(N1−N2−C3−C4)[b]
		water		
$TS_{add.}$	1.84	2.45	2.64	62.0
OI	1.51	2.35	3.10	112.5
$TS_{isomer.}$	1.51	2.13	2.92	94.2
AI	1.55	1.54	2.60	114.0
$TS_{abs.}$	1.49	2.33	2.11	76.0
		methanol		
$TS_{add.}$	1.80	2.47	2.43	46.6
OI	1.50	2.38	3.05	117.0
$TS_{isomer.}$	1.50	2.11	2.65	92.4
AI	1.55	1.55	2.78	104.8
$TS_{abs.}$	1.46	2.43	2.08	20.3
		DMSO		
$TS_{add.}$	1.78	2.48	2.52	71.3
OI	1.52	2.36	3.43	130.2
$TS_{isomer.}$	1.49	2.19	2.88	100.9
AI	1.54	1.53	2.65	112.7
$TS_{abs.}$	1.54	2.00	1.75	70.6
		acetonitrile		
$TS_{add.}$	1.78	2.50	2.62	72.8
OI	1.53	2.32	3.14	121.3
$TS_{isomer.}$	1.50	2.20	2.61	87.2
AI	1.55	1.55	2.78	107.3
$TS_{abs.}$	1.57	1.99	1.77	68.4

[a] From the 2D free-energy maps computed in the QM/MM/MC simulations. $R_1 = R_2 = 5.00$ Å for the reactants. [b] Atom numbering scheme given in Figure 1.

similar results.[13] The angle of tilt of PTAD's 5-membered ring with respect to the alkene plane is ca. 45° for the highly asymmetric transition structure (Figures 4 and S3). This approach maximizes both the electrophilic PTAD-LUMO, tetramethylethylene-HOMO, interaction, and the nucleophilic PTAD-HOMO, tetramethylethylene-LUMO, interaction; a detailed discussion of the frontier orbital interactions operating in the transition structure is given by Chen et al. in ref 12. A favorable electrostatic interaction between the unbound N on PTAD and the allylic hydrogen on tetramethylethylene (R_{NH} in Table 1) was found for $TS_{add.}$ in all solvents computed and is similar to a stabilizing interaction reported between TAD and propene.[12]

The geometries for the transition structure leading to ene product via an allylic proton transfer, $TS_{abs.}$, were found to be significantly more solvent dependent than $TS_{add.}$. In water and methanol, an earlier transition state was computed with reacting bond distances of $R_2 = 2.33-2.43$ Å and $R_{NH} = 2.08-2.11$ Å compared to the aprotic solvents values of $R_2 = 1.99-2.00$ Å and $R_{NH} = 1.75-1.77$ Å (Table 1). The distances between the abstracted allylic hydrogen and its carbon in $TS_{abs.}$ were relatively similar at 1.11, 1.14, 1.19, and 1.17 Å in water, methanol, DMSO, and acetonitrile, respectively. Despite the large differences in the R_{NH} hydrogen abstraction distances, the emerging double bond is similarly formed in protic and aprotic solvents with a predicted bond length of 1.43 Å in both water and DMSO (Figures 4 and S3). The difference in geometries may stem, in part, from the intermediate structures preceding TS_{abs}. However, the major factor dictating the geometry differences and change in reaction path when comparing protic and aprotic solvents is the stabilization of emerging charge separations spanning 2 to 4 atoms in the AI and open intermediates. The relationship between the structures, charges, and energies is discussed below.

Energetics. The computed activation barriers for the ene reaction in solution are summarized in Table 2. Error ranges in the calculated free-energy values have been estimated from fluctuations in the ΔG values for each FEP window using the batch means procedure with batch sizes of 0.5 M configurations.[20] Free-energy changes were obtained with statistical uncertainties ($1\sigma_i$) of only 0.001−0.03 kcal/mol in each window; the overall uncertainties have been derived using the expression $[\sum_i^N \sigma_i^2]^{1/2}$, where N is the number of ΔG_i values. The calculated errors in the free energies imply overall uncertainties in the $\Delta G^{\ddagger}$ values for the transition structures of 0.7 kcal/mol and ΔG of 0.7 kcal/mol for the intermediates, and 0.8 kcal/mol for the product.

The $\Delta G^{\ddagger}$ values predicted from the QM/MM/MC simulations for $TS_{add.}$ are 17.4 and 22.3 kcal/mol in water and methanol, and 13.9 and 14.9 kcal/mol in DMSO and acetonitrile, including a cratic entropy correction of 1.89 kcal/mol to adjust for a 1 M standard state.[36] The experimental $\Delta G^{\ddagger}$ is 19.4 kcal/mol for the reaction between PTAD and *trans*-3-hexene in benzene;[4] correcting for the 2000-fold relative rate enhancement of tetramethylethylene compared to *trans*-3-hexene and using the known rate change upon going from benzene to acetonitrile ($k(CH_3CN)/k(C_6H_6) = 1.2$)[4] allows us to derive a $\Delta G^{\ddagger}$ value of ca. 15.0 kcal/mol for the present reaction in acetonitrile, in excellent quantitative agreement with the calculations. In addition, the reaction has been reported as qualitatively faster in CH_2Cl_2 than in methanol (complete in 4 min versus 10 min at −78 °C),[13] which is also in good accord with the larger activation barrier computed for methanol over the aprotic solvents. The addition of PTAD was found to be rate-limiting in all solvents; however, the traditional mechanism where an AI forms following the initial transition structure is not predicted; instead the reaction proceeds directly to an open intermediate (Figures 2 and 5). Direct formation of an AI intermediate from the reactants is unlikely, as observed in Figures 2 and S1 (in the Supporting Information), as it would require an additional ΔG of ca. 10−15 kcal/mol over that of the barrier leading to the OI. The absolute free energies between the reactants and the AI in Figure 2 have been truncated to a maximum of 50 kcal/mol for clarity, but can be as large as 70 kcal/mol in water. The AI is instead produced by closure of the open intermediate. The activation barrier for the formation of the AI from the open intermediate is significantly lower in the aprotic solvents, 0.8 and 1.2 kcal/mol for DMSO and acetonitrile, compared to the protic solvents, 5.5 and 3.2 kcal/mol in water and methanol. The results suggest the lifetime of the open intermediate in the aprotic solvents may be smaller than the 10^{-11} s needed for detection via the cyclopropyl probe used in the study by Roubelakis et al.,[11] which shows activation energies of more than 2.0 kcal/mol for the opening of phenyl-substituted cyclopropylcarbinyl radicals.[37] Thus, these calculations explain why the characteristic ring-opened products were not observed in acetonitrile and DMSO, but were the major products in methanol and ethanol.[11]

An unresolved issue pertaining to the ene mechanism is the likelihood of partial reversion of the intermediates to starting material. Intermediate reversal has been proposed to explain a significant intramolecular kinetic isotope effect observed be-

(36) (a) Yu, B. Y. *J. Pharm. Sci.* **2001**, *90*, 2099−2102. (b) Hermans, J.; Wang, L. *J. Am. Chem. Soc.* **1997**, *119*, 2707−2714.

(37) Newcomb, M.; Johnson, C. C.; Manek, M. B.; Varick, T. R. *J. Am. Chem. Soc.* **1992**, *114*, 10915−10921.

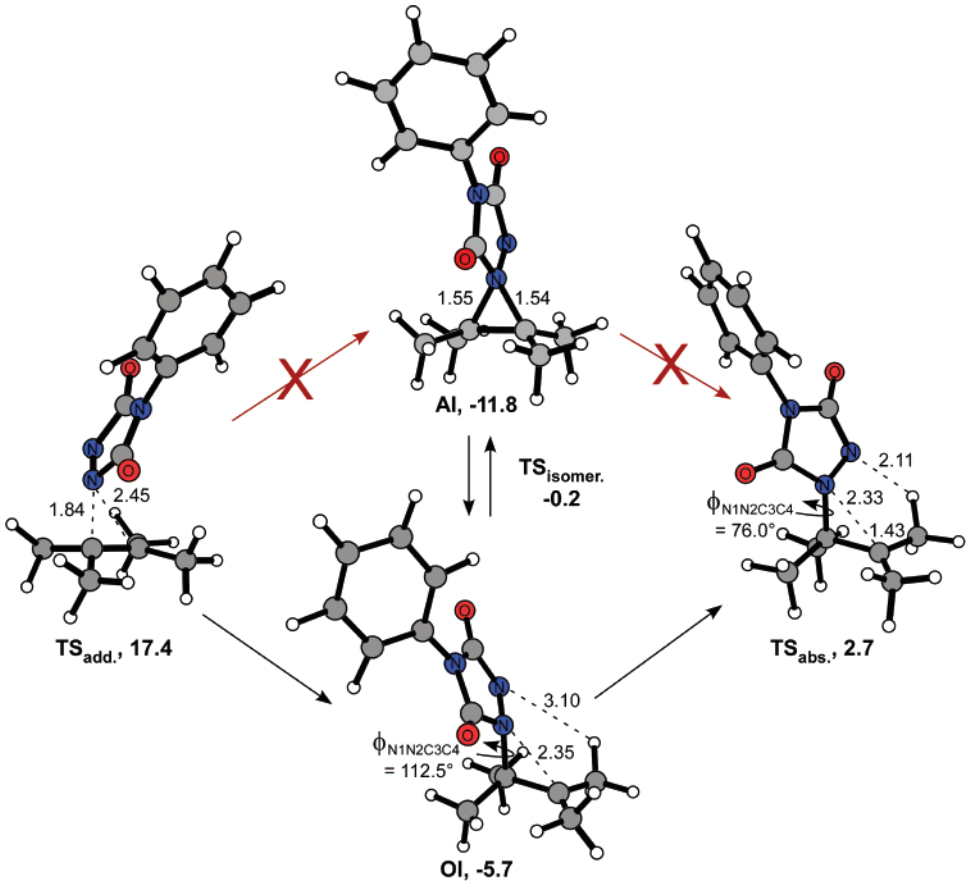

FIGURE 4. Optimized structures for the ene reaction between 4-phenyl-1,2,4-triazoline-3,5-dione (PTAD) and tetramethylethylene in water from QM/MM/MC simulations (abbreviations given in Figures 2 and 3). All distances are in angstroms and free energies (shown in bold) relative to the reactants are in kcal/mol.

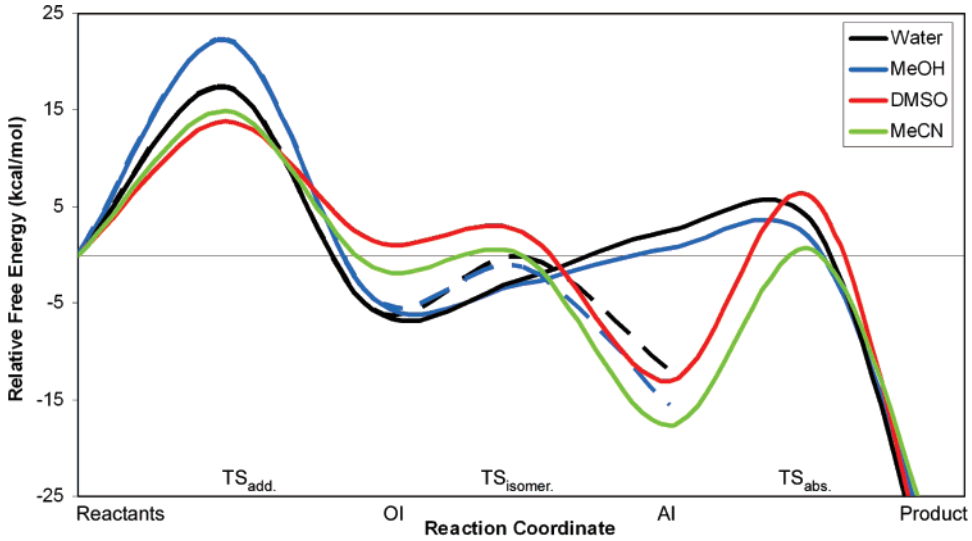

FIGURE 5. Free-energy profiles for the ene reaction between PTAD and tetramethylethylene in the four solvents from the QM/MM/MC calculations. Solid lines represent the minimum energy pathway toward product and dashed lines indicate an equilibrium occurring in the protic solvents between the intermediates.

tween PTAD and *trans*-d_3-2-butene.[7,35] Subsequent studies have questioned the validity of a reversion occurring due to a lack of reactant formation from the decay of an isolated AI between MTAD (M = methyl) and cycloheptene,[16] and the comparison of computed energy profiles to calculated and experimentally measured kinetic isotope effects for various TAD−olefin reactions.[12,13] The AI is presently calculated to be the lowest energy intermediate in all four solvents, coinciding with the stability needed for spectroscopic observation.[6,9,15] The QM/MM/MC simulations suggest that reversion of formation of the AI to starting material is unfavorable, at least in the case of tetramethylethylene, as the computed $\Delta G^{\ddagger}_{reversion}$ in water,

TABLE 2. Free-Energy Changes, ΔG (kcal/mol), at 25 °C for the Ene Reaction between PTAD and Tetramethylethylene Using PDDG/PM3/MM/MC

	water[a]	MeOH[a]	DMSO[b]	CH_3CN[b]
reactants	0	0	0	0
$TS_{add.}$	17.4	22.3	13.9	14.9
OI	−5.7	−4.5	1.5	−1.3
$TS_{isomer.}$	−0.2	−1.3	2.3	−0.1
AI	−11.8	−15.5	−13.0	−17.7
$TS_{abs.}$	2.7	0.9	5.4	0.2
product	−47.7	−41.3	−48.7	−39.6

[a] OI leads to product. [b] AI leads to product. Experimental $\Delta G^{\ddagger}$ (kcal/mol) for $TS_{add.}$ = ca. 15.0 in CH_3CN.[4]

TABLE 3. B3LYP/6-311++G(2d,p)/CPCM Results for $\Delta G^{\ddagger}$ (kcal/mol) at 25 °C for the Ene Reaction between PTAD and Tetramethylethylene[a]

	water[a]	MeOH[a]	DMSO[b]	CH_3CN[b]
reactants	0	0	0	0
$TS_{add.}$	24.6	25.6	25.0	24.0
OI	19.5	20.7	20.0	19.1
$TS_{isomer.}$	20.3	21.4	20.8	19.8
AI	17.2	18.3	17.7	16.7
$TS_{abs.}$	21.1	22.3	21.6	20.7
product	−11.1	−10.1	−10.6	−11.6

[a] Single point calculation on B3LYP/6-31+G(d) optimized geometries and vibrational frequencies. [b] Experimental $\Delta G^{\ddagger}$ (kcal/mol) for $TS_{add.}$ = ca. 15.0 in CH_3CN.[4]

methanol, DMSO, and acetonitrile, 29.2, 37.8, 26.9, and 32.6 kcal/mol, is sufficiently large to impede an equilibrium. The origin of the large intramolecular kinetic isotope effects has also been attributed to a stabilizing electrostatic interaction between the unbound N on PTAD and the allylic hydrogen on the alkene at the rate-determining transition state.[12] While the same interaction is found in the present calculations for all four solvents (R_{NH} in Table 1), theoretically computed kinetic isotope effects on the rate-limiting transition structure by Singleton and Hang gave values of 1.12 and 1.15 using HF and B3LYP,[13] which is significantly lower than the 1.25 measured experimentally.[7,35] Another possible rationalization for the observed interaction is if the equilibrium between the open intermediate and the AI is more rapid than product formation or C−N bond rotation. The QM/MM/MC simulations find that the activation barrier for isomerization between the open and AI intermediates, $TS_{isomer.}$, is slightly lower than ene adduct formation, $TS_{abs.}$ (see Table 2); however, a C−N rotation between both open intermediates bypassing the AI entirely was not carried out.

The absolute $\Delta G^{\ddagger}$ values for the allylic hydrogen abstraction, $TS_{abs.}$, are significantly lower than the rate-determining step. Experimental activation energies measured for ene product formation from an isolated AI for the reactions of *trans*-cycloheptene in dimethyl ether (13.4 kcal/mol)[6] and *trans*-cyclooctene in CD_2Cl_2 (16.2 kcal/mol)[9] are in good quantitative agreement with the calculated $\Delta G^{\ddagger}$ values relative to the AI: 14.5, 16.4, 18.4, and 17.9 in water, methanol, DMSO, and acetonitrile. The protic solvents are predicted to give lower activation barriers, $TS_{isomer.}$, for the isomerization from AI to the open intermediate, with free energy values relative to the AI of 11.6 and 14.2 kcal/mol in water and methanol compared to 15.3 and 17.6 kcal/mol in DMSO and acetonitrile. In addition, the open intermediate is more stable in protic compared to aprotic solvents, implying greater stabilization derived from a hydrogen-bonding environment.

Continuum Solvent Models. Limited solvation calculations using the implicit SCIPCM solvent model on B3LYP and Hartree−Fock (HF) optimized transition structures for the reaction between TAD and 2-methyl-2-butene have been reported.[13] A slight increase in the activation barrier (0.1 kcal/mol) going from benzene to acetonitrile was predicted using density functional theory (DFT) in reasonable accord with the insensitivity of the rates for TAD reacting with 2-methyl-2-butene in solvents of differing polarities;[2,4] the reaction mechanism or intermediate stabilities were not explored in the solution-phase calculations. In light of the mechanistic implications of solvent, new calculations were carried out using the conductor-like polarizable continuum model (CPCM) in conjunction with DFT on the present system in order to directly compare with the QM/MM/MC results and experiment. This DFT/CPCM approach has been shown to provide good accuracy for computing free energies of hydration for a variety of organic molecules and ions.[38] Transition structures, intermediates, and ground states were initially located in vacuum at the restricted and unrestricted B3LYP/6-31+G(d) level. A vibrational analysis of the $TS_{add.}$ structure gives an imaginary frequency with transition vectors showing the attacking PTAD nitrogen undergoing bond formation with a single carbon atom from tetramethylethylene, suggesting that the transition state leads directly to an open intermediate. A similar result was computed for TAD and propene by Singleton and Hang[13] and found in the present QM/MM/MC simulations.

Single-point energy calculations with a larger basis set, 6-311++G(2d,p), were then executed in four different solvents using the CPCM method to yield the $\Delta G^{\ddagger}$ values in Table 3. A 1.89 kcal/mol correction was included in the calculations to account for change in the standard state from 1 atm to 1 M.[36] The DFT/CPCM method correctly predicts $TS_{add.}$, the addition of PTAD, as rate-limiting, but the $\Delta G^{\ddagger}$ values are overestimated compared to experiment. In addition, the continuum model fails to reproduce observed changes in the rate of the reaction in solvents with increasing polarity. For example, the reaction between PTAD and tetramethylethylene proceeds 5.5 times faster in acetonitrile over methylene chloride,[4] but DFT/CPCM predicts the reaction to have similar activation energies in all four solvents computed (Table 3). The DFT/CPCM calculations also underestimate the activation barrier of ene product formation from the AI intermediate, with energy values of 3.9, 4.0, 3.9, and 4.0 kcal/mol in water, methanol, DMSO, and acetonitrile compared to experimental values of 13.4 and 16.2 kcal/mol for related ene reactions.[6,9] Specific changes in hydrogen bonding are expected to be important along the reaction path, but they are not explicitly treated in the continuum treatment. Similar problems differentiating $\Delta G^{\ddagger}$ values between protic and aprotic solvents using continuum solvent models have been reported for various organic reactions, e.g., Diels−Alder,[27] Cope elimination,[25] and nucleophilic aromatic substitution reactions.[23] The QM/MM/MC calculations with their explicit representation of the solvent molecules overcome this limitation (Table 2).

Zwitterion or Diradical? Unrestricted B3LYP calculations were also carried out for the open intermediate; a computed $\langle S^2 \rangle$ of 0.32 and a Mulliken spin density of 0.55 on the unbound olefinic carbon are suggestive of a diradical nature, $\langle S^2 \rangle = 1.00$. However, a negligible ΔG difference was computed between the restricted and unrestricted calculations for the gas-phase open intermediate, 23.2 and 23.1 kcal/mol, showing that although a

(38) Takano, Y.; Houk, K. N. *J. Chem. Theory Comput.* **2005**, *1*, 70−77.

TABLE 4. CHELPG Charges for the Ene Reaction between PTAD and Tetramethylethylene[a]

	$TS_{add.}$	OI	$TS_{isomer.}$	AI	$TS_{abs.}$
			water		
N1	−0.636	−0.748	−0.775	−0.775	−0.657
N2	−0.090	0.073	0.114	0.239	−0.103
C3	0.216	0.340	0.377	0.293	0.294
C4	0.263	0.287	0.237	0.270	0.312
			methanol		
N1	−0.633	−0.743	−0.770	−0.772	−0.651
N2	−0.037	0.076	0.113	0.237	−0.102
C3	0.212	0.345	0.385	0.288	0.295
C4	0.257	0.272	0.218	0.266	0.304
			DMSO		
N1	−0.633	−0.743	−0.770	−0.771	−0.651
N2	−0.087	0.076	0.112	0.237	−0.102
C3	0.210	0.345	0.388	0.291	0.295
C4	0.256	0.272	0.208	0.256	0.304
			acetonitrile		
N1	−0.634	−0.744	−0.770	−0.772	−0.649
N2	−0.086	0.078	0.112	0.238	−0.102
C3	0.210	0.348	0.390	0.288	0.294
C4	0.255	0.267	0.211	0.261	0.302

[a] From B3LYP/6-311++G(2d,p)//B3LYP/6-31+G(d)//CPCM calculations. Atom numbering scheme given in Figure 1.

TABLE 5. CM3 Charges for the Ene Reaction between PTAD and Tetramethylethylene[a]

	$TS_{add.}$	OI	$TS_{isomer.}$	AI	$TS_{abs.}$
			water		
N1	−0.478	−0.755	−0.742	−0.791	−0.758
N2	−0.131	−0.210	−0.151	0.220	−0.261
C3	0.140	0.151	0.151	0.081	0.168
C4	0.005	0.502	0.350	0.065	0.481
			methanol		
N1	−0.476	−0.736	−0.737	−0.792	−0.862
N2	−0.030	−0.222	−0.189	0.223	−0.206
C3	0.083	0.161	0.162	0.063	0.201
C4	0.028	0.441	0.397	0.057	0.459
			DMSO		
N1	−0.450	−0.695	−0.718	−0.814	−0.795
N2	−0.026	−0.266	−0.090	0.295	−0.083
C3	0.090	0.133	0.189	0.032	0.207
C4	−0.017	0.520	0.290	0.058	0.228
			acetonitrile		
N1	−0.386	−0.704	−0.759	−0.826	−0.769
N2	−0.025	−0.276	−0.149	0.262	−0.166
C3	0.059	0.110	0.191	0.068	0.181
C4	−0.078	0.509	0.334	0.057	0.226

[a] From QM/MM/MC simulations. Atom numbering scheme given in Figure 1.

diradical nature for this intermediate is unlikely, a gas-phase polarized diradical species cannot be ruled out. Further, single-point calculations including solvent effects on the open intermediate using UB3LYP/6-311++G(2d,p)/CPCM gave ΔG values identical with the restricted values reported in Table 3, suggesting any diradical character present for the OI in the gas phase becomes highly polarized when the OI is solvated. The AI is predicted to be the lowest energy intermediate in the four continuum solvents computed with an average energy value of 19.4 kcal/mol, which is close to the average energy for the open intermediate, 21.7 kcal/mol; the similarity between the open and AI intermediate energies appears to be an artifact of the DFT/CPCM calculations. Unlike the QMM/MM/MC calculations where free-energy maps (Figures 2 and 3) can be readily used to determine the reaction pathway (Figure 5), the DFT/CPCM calculations simply give the absolute energy values of stationary points on the reaction profile, making predicting the overall effect of solvent on the mechanism difficult.

To further investigate the zwitterionic versus diradical controversy, atomic charges have been computed for all stationary points along the reaction path. Mulliken charges were previously computed for the gas-phase reaction between 2-methyl-2-butene and TAD using B3LYP calculations;[13] a moderate charge separation of ca. 0.5 e in the open intermediate was presented as evidence for a diradical pathway, as a zwitterion would be expected to have a much larger charge separation. New calculations on the present system were carried out using the CHELPG charge model[39] and (U)B3LYP/6-311++G(2d,p) single points in the gas phase and in CPCM solvent (Table 4; the abbreviations N1, N2, C3, and C4 are defined in Figure 1). CHELPG charges set in an all-atom format have previously been shown to be more reliable than the Mulliken charges in solvent simulations.[40] In the gas phase, a charge separation of 0.811 and 0.763 e was computed for the open intermediate using the restricted and unrestricted DFT methods, respectively. The charge separation was found to be greatly enhanced in solution, confirming that any diradical character present in the open intermediate may only exist in gas. The charge separation computed for the AI zwitterions (between atoms N1 and N2), 1.01, 1.01, 1.01, and 1.01 e in water, methanol, DMSO, and acetonitrile, is nearly identical with that of the open intermediate, with values of 1.04, 1.02, 1.02, and 1.01 e (between atoms N1 and C4). In addition, the computed dipole moment for the open intermediate using both restricted and unrestricted DFT also shows a much larger charge separation present in solution when compared to gas, with a gas-phase value of 5.80 debye and solution-phase dipole moments of 9.35, 9.22, 9.24, and 9.22 debye in water, methanol, DMSO, and acetonitrile, respectively.

CM3 charges were also computed using the QM/MM/MC method from the final configuration sampled for the transition states and intermediates, which have been determined to be good representations of the average structures.[26] Partial charges are reported in Table 5 for the reacting nitrogen and carbon atoms on PTAD and tetramethylethylene. The computed charge separation between N1 and N2 for the AI is 1.01, 1.02, 1.11, and 1.09 e and that between N1 and C4 for the open intermediate is 1.26, 1.18, 1.22, and 1.21 e in water, methanol, DMSO, and acetonitrile, respectively. The QM/MM/MC derived CM3 charges are in good agreement with the DFT CHELPG charges. Both methods are indicative of a dipolar intermediate in solution, which should address any concerns about an inconsistent treatment for a biradical system with the PDDG/PM3 semiempirical method. Experimental observations on PTAD−alkene reactions using a cyclopropylcarbinyl probe to distinguish between biradical and dipolar open intermediates also strongly support the exclusive formation of a 1,4-dipolar intermediate.[11]

Solvent Effect on the Rate of Reaction. While solvent effects on the rates of reaction for PTAD with alkenes are generally small,[2,14] reduced rates in THF and ethyl acetate over other solvents, including benzene, have been consistently observed for multiple ene reactions.[14] The results led Ohashi and Butler to measure the visible absorption of PTAD in various solvents and they found λ_{max} of PTAD in THF and ethyl acetate

(39) Breneman, C. M.; Wiberg, K. B. *J. Comput. Chem.* **1990**, *11*, 361−373.

(40) Carlson, H. A.; Nguyen, T. B.; Orozco, M.; Jorgensen, W. L. *J. Comput. Chem.* **1993**, *14*, 1240−1249.

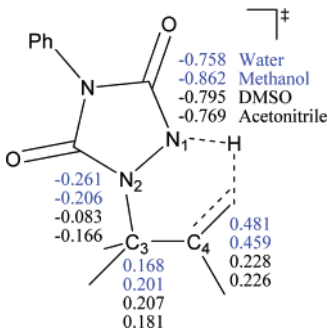

FIGURE 6. Selected atomic CM3 charges for the transition structure leading toward ene product, $TS_{abs.}$, for the reaction between PTAD and tetramethylethylene in water and methanol (colored in blue) and DMSO and acetonitrile (colored in black) using PDDG/PM3.

to be lower by 15 nm over benzene.[14] It was rationalized that a strong donor−acceptor complex interaction between PTAD and the solvent may be responsible for the lower reactivity, possibly due to an increase in the electron density at the N═N PTAD atoms. As noted previously, hydrogen bonding is sensitive to small charge shifts.[26,27] Computed CM3 charges using PDDG/PM3 on PTAD's N1 and N2 atoms gave values of −0.099 and −0.087 e in the gas phase, −0.094 and −0.078 e in acetonitrile, −0.089 and −0.089 e in DMSO, −0.081 and −0.046 e in methanol, and −0.117 and −0.112 e in water, confirming a general increase in N═N charge density with increasing solvent polarity, which agrees with the calculated activation barrier increase for $TS_{add.}$ in the protic solvents (Table 2).

Once the open intermediate has formed, the rate of ene product formation is expected to be faster in protic over aprotic solvents when comparing the computed activation barriers for $TS_{abs.}$ in the different media (see Table 2 and Figure 5). This trend can be attributed to an enhanced stability, via hydrogen bonding, of the pronounced charge separations for $TS_{abs.}$ in the protic solvents. Accordingly, the CM3 charges computed for $TS_{abs.}$ (Figure 6) show the charges become more negative at the N1 and N2 atoms and the amount of positive charge on the C4 atom doubles in protic solvents compared to that in aprotic solvents.

Solvation. Detailed insight on the changes in solvation along the reaction pathways are available from the present QM/MM/MC calculations. Specifically, the solute−solvent energy pair distributions record the average number of solvent molecules that interact with the solute and the associated energy. The interaction energies are quantified by analyzing the QM/MM/MC results in five representative FEP windows: near the reactants, the AI and open intermediates, and the addition and product-forming transition structures. The results for the ene reaction in water and acetonitrile are shown in Figure 7 (the results for methanol and DMSO are given in Figure S4 of the Supporting Information). Hydrogen bonding in water and the most favorable electrostatic interactions in acetonitrile are reflected in the left-most region, with solute−solvent interaction energies more attractive than −5 kcal/mol. The large bands near 0 kcal/mol result from the many distant solvent molecules in outer shells.

Of relevant interest is the exact nature of the favorable solute−solvent interactions in relation to the emerging charge separations in AI and open intermediates. It is immediately clear in viewing Figures 7 and S4 that the open intermediate has

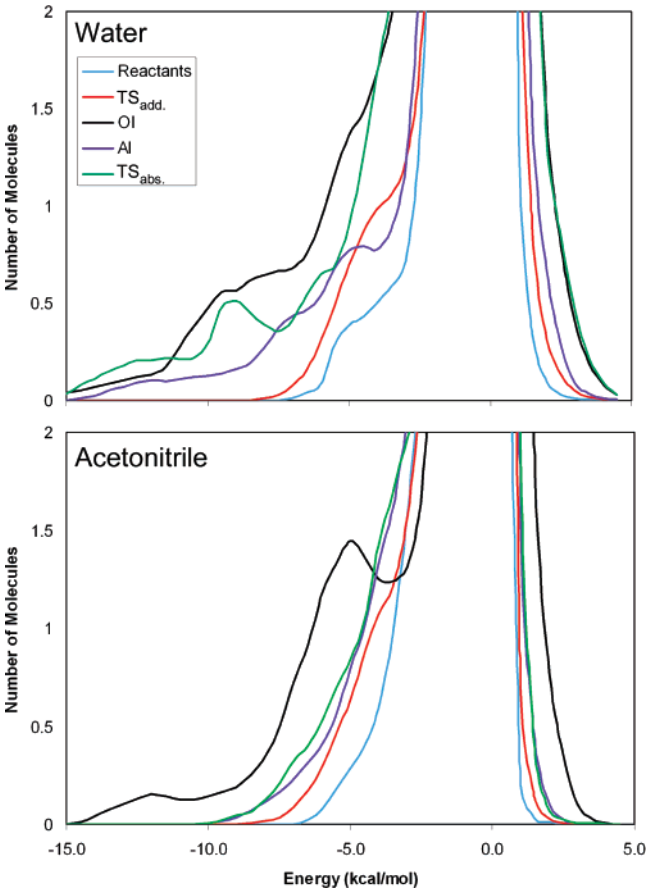

FIGURE 7. Solute−solvent energy pair distributions for the reaction between PTAD and tetramethylethylene in water and acetonitrile for the reactants, transition structures ($TS_{add.}$ and $TS_{abs.}$), aziridinium imide (AI), and open intermediate (OI). The ordinate records the number of solvent molecules that interact with the solutes with their interaction energy on the abscissa. Units for the ordinate are number of molecules per kcal/mol.

stronger bands compared to the AI in all solvents. Integration of these bands to a cutoff energy of −4.0 kcal/mol yields 13.0 and 6.4 water molecules, 10.4 and 4.3 methanol molecules, 10.7 and 6.8 DMSO molecules, and 10.7 and 5.1 acetonitrile molecules for the open intermediate and AI, respectively. The weaker solute−solvent energy bands for both intermediates in acetonitrile compared to water suggest it stems from the aprotic solvents' inability to properly stabilize a charge separation. From the display of configurations such as in Figure 8, on average there is one short, strong N···H hydrogen bond and one long hydrogen bond with water molecules and the unbound N in the AI, whereas the extended structure of the open intermediate allows for two short, strong hydrogen bonds and one longer one. The remaining strongly attractive interactions are between water and the oxygens on PTAD and a π-type hydrogen bond with the phenyl ring. Hydrogen bonding plays an important role in determining the equilibrium between the open and AI intermediates. The increased stabilization of the open intermediate in protic solvents is due to enhanced solvent accessibility to the strong dipolar character of the unbound nitrogen and carbon in the open intermediate (−0.755 and 0.502 e) compared to the nitrogen atoms in the AI (−0.791 and 0.220 e). The increased solvent accessibility also allows for stronger electrostatic interactions with acetonitrile, but the additional stabilization is not enough to compensate for the increasingly unfavor-

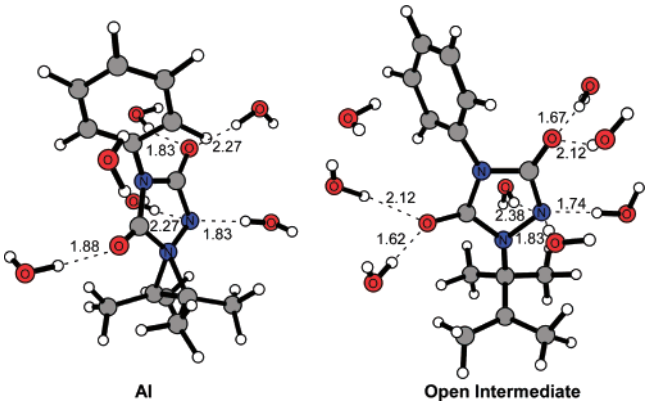

FIGURE 8. Typical snapshot for the AI and open intermediates from the ene reaction between PTAD and tetramethylethylene in water (only nearest water molecules are illustrated). Distances in angstroms.

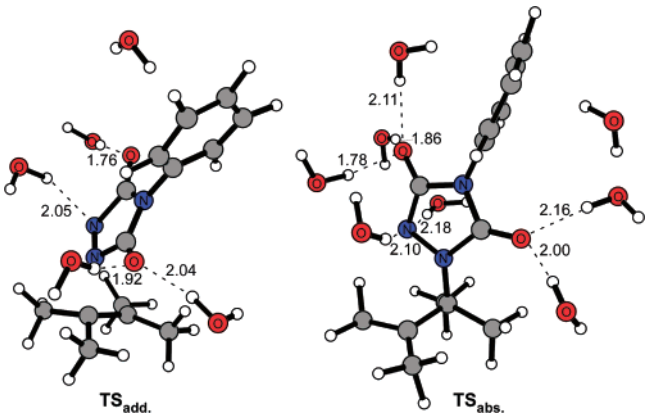

FIGURE 9. Typical snapshot for the transition structures from the ene reaction between PTAD and tetramethylethylene in water (only nearest water molecules are illustrated). Distances in angstroms.

able energy associated with the large charge separation distances in the open intermediate compared to the 1,2-dipole in the AI.

Stronger hydrogen bond interactions at the product-forming transition state ($TS_{abs.}$ in Figures 7 and 9) are consistent with the computed reduction of the activation barrier in the protic solvents compared to the aprotic solvents. For example, the lower energy bands for the second transition structure, $TS_{abs.}$, in acetonitrile reflect less favorable interactions compared to those of the strong hydrogen bonds in water. Integrating the energy bands to a cutoff energy of −4.0 kcal/mol reveals 3.6 and 10.2 water molecules, 3.6 and 5.7 acetonitrile molecules, 2.5 and 9.0 methanol molecules, and 4.3 and 7.8 DMSO molecules interacting with $TS_{add.}$ and $TS_{abs.}$, respectively.

The solute−solvent structure for the PTAD−tetramethylethylene reaction in water can be further characterized by radial distribution functions, $g(R)$. Hydrogen bonding between the unbound nitrogen of PTAD and the hydrogens of water, N1(PTAD)−H(water), should yield contacts shorter than 2.5 Å. The corresponding $g_{N1-H}(R)$ gives the probability of finding a hydrogen of water at a distance of R from N1. Accordingly, the ene reaction shows a well-defined first peak, with the exception of the reactants, centered around 1.9 Å with a minimum around 2.7 Å that reflects the hydrogen bonds (Figure 10). Hydrogen bonding is clearly the greatest for the AI and open intermediates, corresponding to their large charge separations. The amount of hydrogen bonding falls slightly for $TS_{abs.}$, consistent with the charge decrease on N1 as the allylic hydrogen is transferred to PTAD. The initial transition structure, the addition of PTAD, has greatly reduced hydrogen bonding and the reactant PTAD has virtually no hydrogen bond interactions at the nitrogen position. The low radial distribution function for $TS_{add.}$ reflects a small but significant solvent effect on the rate-determining addition step as seen in the calculated energies of $TS_{add.}$ (Table 2).

Integration of the first peaks to a minima of near 2.7 Å yields averages of 2.7 and 2.2 hydrogen bonds between N1 of PTAD and water molecules for the open intermediate and AI, respectively. This is well-illustrated in Figure 8, showing a snapshot of the open intermediate with two tight hydrogen bonds and one slightly longer, and two water molecules complexed to N1 of PTAD in the AI. Integrating the first peak for the product-forming transition structure to the same minima yields an average of 2.4 hydrogen bonds. Figure 9 depicts the water molecules hydrogen bonded to N1 on $TS_{abs.}$ with slightly longer bonds compared to the open intermediate. So while the solvent accessibility of water is similar for $TS_{abs.}$ and the open intermediate, the strength of the hydrogen bond is reduced in agreement with the energy pair distributions and the radial

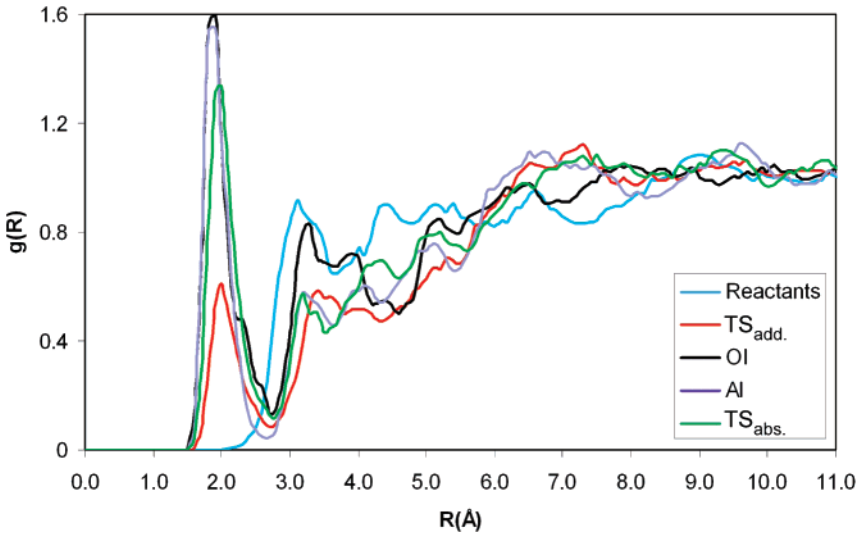

FIGURE 10. Computed N1(PTAD)−H(water) radial distribution functions for the reaction between PTAD and tetramethylethylene at 25 °C.

distribution functions. Similar results were found for methanol. The large $g(R)$ peak in Figure 10 for $TS_{abs.}$ is indicative of enhanced interactions between water and the transition structure and indicates that greater solvent accessibility may be responsible for the change in the reaction mechanism. In protic solvents an open transition structure is better stabilized via hydrogen bonding with the reaction medium, hence the abstraction occurs from the open intermediate, while a more closed transition structure is preferred in the absence of hydrogen bonding and abstraction occurs via the AI.

Conclusions

QM/MM/MC simulations have been carried out to elucidate the effects of solvation on the controversial triazolinedione ene mechanism. Calculations for the reaction between PTAD and tetramethylethylene in water, methanol, DMSO, and acetonitrile are in good quantitative accord with experimentally measured free energies of activation. A stepwise mechanism was confirmed and the addition of PTAD to the alkene was found to be the rate-determining step. The traditional mechanism where an AI forms following the rate-limiting transition structure was not found. Instead, the calculations predict the reaction proceeds directly to an open intermediate. The activation barrier preceding the formation of the AI from the open intermediate is significantly smaller in the aprotic solvents, thus explaining the solvent effects observed in the ene reaction of cyclopropyl-substituted alkenes. Reversion of the intermediates to starting material was found to be unfavorable in all solvents.

Similarities exist between the present results and the biradical mechanism proposed by Singleton and Hang; however, pronounced charge separations computed in solution strongly support the exclusive formation of an open dipolar intermediate and not a biradical species. Analysis of solute−solvent interactions and charges suggests that larger activation barriers in the protic solvents compared to aprotic solvents may stem from greater stabilization of the electron density at the N═N atoms in PTAD in the reactants. The most significant solvent effect reported is a change in the reaction pathway for the formation of the ene product in protic and dipolar aprotic solvents; the reaction proceeds through the AI intermediate in aprotic solvents or an open intermediate in protic solvents. A reduced activation barrier in the aprotic solvents and change in mechanism toward the final ene adduct is the result of enhanced hydrogen bond stabilization of the large charge separations prevalent in the open intermediate and product-forming transition structure.

The findings have significant impact for predicting the effect of solvation on the mechanism for similar and related ene reactions. Other potentially productive possibilities include manipulation of intermediate equilibrium balances geared toward open intermediate detection and enhancing stereoselective product outcomes by changing solvent polarity.

Acknowledgment. Gratitude is expressed to the Alabama Supercomputer Center and Auburn University for support of this research.

Supporting Information Available: Illustration of optimized structures in DMSO from QMM/MM/MC simulations; free-energy maps for the reaction in methanol and acetonitrile; additional solute−solvent energy pair distributions for methanol and DMSO; energies, frequencies, and coordinates of all structures computed using DFT/CPCM; and complete ref 33. This material is available free of charge via the Internet at http://pubs.acs.org.

JO7022153